



NEW CONCEPTS IN MODELING DAMPING IN STRUCTURES

Adam Bowland¹, Finley Charney², Cristopher D. Moen³ and Jordan Jarrett⁴

ABSTRACT

Most current methods for modeling damping in structures assume global linear viscous damping, even when nonlinear behavior is present in the structural system. While this approach is easy to implement, the results do not accurately model the displacement-history dependent damping behavior that is inherent in damaged members, nonstructural components and connections. This work presents a new method for modeling damping that can account for the nonlinearity of damping behavior across the system. In this method damping is added to each individual element or connection through the use of ghost elements, wherein a variety of damping springs are used to account for energy dissipation. In the work presented in this paper, the springs dissipate energy through rotation, and phenomenological rules are used to determine the damping moments in the in the springs. Two sets of rules are described; evolutionary and microscale. The evolutionary model is based on the concept of nonlinear viscous damping, and the microscale model uses experimentally determined energy dissipation relationships to model the damping. Although these methods increase computational demands for the nonlinear analysis of structures, the versatility of the approach allows for modeling a wide range of behavior that is not possible with the traditional global linear viscous damping models.

Introduction

Damping is one of the most important but least understood parameters in the dynamic response history analysis of structures. Contributing to the lack of understanding are broad uncertainties in identifying the physical damping mechanism and in quantifying the magnitude of damping. These uncertainties have led to the development of ad-hoc methods for including damping in structural analysis. Most of these methods are based on the concepts of spatially uniform constant linear viscous damping, although it is generally recognized that the principal mechanism for damping is not viscous, varies throughout the structure, and changes during the response.

¹ Graduate Research Assistant, Dept. of Civil Engineering, Virginia Tech, Blacksburg, VA 24061

² Associate Professor, Dept. of Civil Engineering, Virginia Tech, Blacksburg, VA 24061

³ Assistant Professor, Dept. of Civil Engineering, Virginia Tech, Blacksburg, VA 24061

⁴ Graduate Research Assistant, Dept. of Civil Engineering, Virginia Tech, Blacksburg, VA 24061

The traditional approach to include damping in nonlinear structural analysis is to form a damping matrix, C . This matrix is usually formed as a linear combination of mass, M , and stiffness, K , as follows

$$C = a_0 M + a_1 K \quad (1)$$

This form of C , which is not physically related to any actual damping mechanism in a structure, was initially developed to preserve linearity in the system and to allow uncoupling of the equations of motion. It is curious that the method has persisted in the analysis of inelastic systems, wherein linearity is not required and modal uncoupling is not practical.

Regardless of its shortcomings, the damping matrix developed from Eq. 1 works reasonably well for lightly damped linear systems. However, several researchers (Bernal 1994; Charney 2008; Chrisp 1980; Hall 2006; Powell 2008) have questioned the validity of Eq. 1 when nonlinear analysis is used. The fundamental concern is that changes in system frequencies can result in changes in the effective damping ratios, particularly if the damping matrix is based on the initial stiffness of the system. Most of the suggested "fixes" for this problem are based on refinements to the proportional damping concept (e.g. using instantaneous tangent stiffness instead of initial stiffness in Eq.1) and thereby still rely on the concepts of linear viscous damping. Ultimately, these fixes are bound to fail, because the fundamental problem has not been addressed.

The remainder of this paper presents two implementations for a new approach for modeling damping in nonlinear dynamic analysis. In each case physical analogues for energy dissipation in materials and components are modeled directly and are applied at the material, element, or component level. The first of these two methods is a discrete "evolutionary" model, in which the energy dissipation is represented by phenomenological damping elements whose deformation field is constrained to be the same as the deformation field for the primary element to which they are attached. A simple nonlinear viscous damping model is used for these elements, and together with sets of associated rules, the character of the damping in these elements may transform, for example, from linear viscous to Coulomb. The second approach, called a microscale approach (because it is applied, in essence, at the micro-material level), is based on hysteretic energy dissipation relationships developed by Lazan (1968).

Evolutionary Model

In the proposed model, structural damping is added to each element through rotational dampers that are attached to rigid-link ghost elements which are constrained to the structural element (Figure 1). The deformations along the length of the structural element are transformed into rotations at the hinges of the rigid-links and into the damping elements.

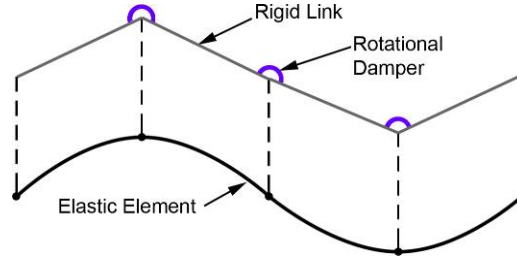


Figure 1. Rigid link model with rotational dampers.

The rotational dampers are modeled with a viscous nonlinear damping model described by Eq. 2

$$f_d = C \text{sign}(\dot{u}) |\dot{u}|^\alpha \quad (2)$$

Where f_d is the force (moment) in the damper, \dot{u} is the rotational velocity in the damper, C is a coefficient of damping, $\text{sign}(\dot{u})$ is the signum function that returns -1 or 1, and α describes the shape of the curve. Figure 2a illustrates different force velocity relationships that are generated by modifying C and α . The dampers can be modeled as viscous ($\alpha = 1.0$), may behave similar to Coulomb damping ($\alpha \leq 0.2$) or provide increased damping as velocity increases ($\alpha \geq 1.0$). Using this model, the damping in any structural element can be changed during an analysis by simply modifying the values of C and α .

For any α value other than 1.0, numerical problems arise when velocities are close to zero. When $\alpha < 1.0$, the effective damping, or tangent, of the curve approaches infinity as the velocity approaches zero. When $\alpha > 1.0$, the effective damping approaches zero as velocity nears zero. Both cases present convergence problems for dampers when the instantaneous velocity is small. This problem is handled by assuming the force-velocity relationship is linear when the velocity is close to zero, less than 0.005 radians per second for instance.

The effects that C and α can have on the damping of a structural element can be illustrated with the free vibration response of a cantilevered column. The column in this example has a length of 144 in., modulus of elasticity of 30,000 ksi, moment of inertia of 1728 in.⁴ and mass per unit length of 0.05 kip second squared per inch. The column has modal periods of 0.70 seconds in the first mode and 0.11 seconds in the second mode. The rigid-link ghost column is modeled with three rotational dampers similar to Figure 1, where each damper has identical properties.

Four different force-velocity damping relationships are used: $\alpha = 1.5$, $\alpha = 1.0$, $\alpha = 0.6$, and $\alpha = 0.2$. Each column is independently deformed into both its first and second mode shapes, released, and then allowed to vibrate freely. The initial deformation is scaled such that the displacement at top of the column is one inch in all analyses. In order to compare results, the damping coefficients associated with each value of α are proportioned on the basis of the equal energy concept described by Hanson and Soong (2001). The purpose of this scaling is to use damping coefficients such that the energy dissipated per cycle of vibration is equivalent in each

damper (Figure 2b) for a given frequency and single vibration amplitude. For this analysis, the damping coefficients are calculated using the frequency and maximum damper rotations of the first mode. The damping coefficients associated with each α value are shown in Figure 2.

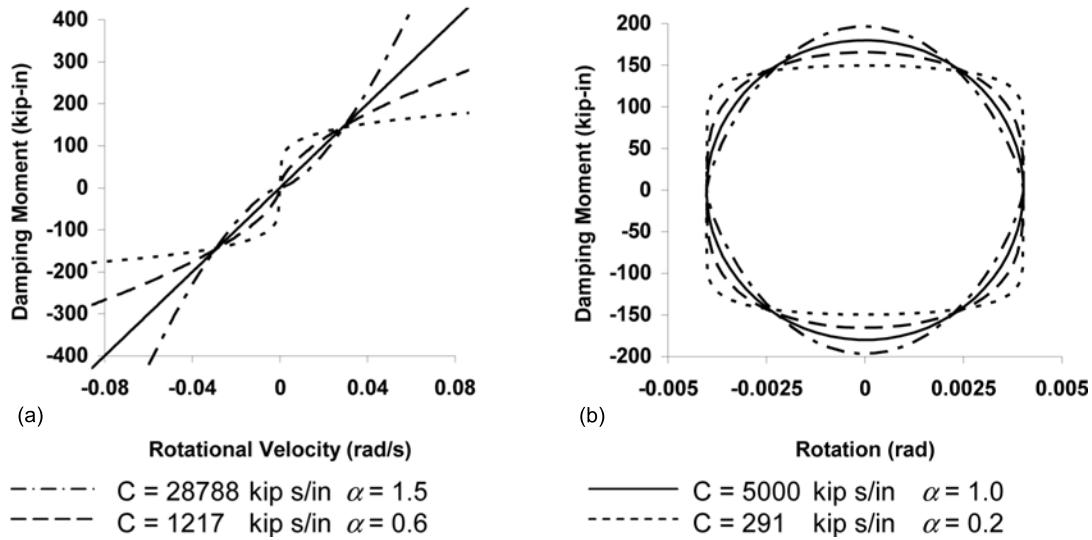


Figure 2. Linear and nonlinear damping models: (a) damping force vs. velocity and (b) damping force vs. displacement.

Each analysis is performed using a Newmark constant acceleration time stepping scheme. For the nonlinear damping models, the solution at each timestep is solved by iterating on the damping forces until an equilibrium force imbalance of 0.1 kips is achieved. The lateral displacements at the top of the column are plotted for all four analyses in Figure 3. The responses in the second mode are separated for clarity.

For the first eight cycles in the mode 1 response, all three models provide very similar damping. This is because the dampers are calibrated to be equivalent at this amplitude and frequency of vibration. As the vibration amplitude begins to decrease, however, the $\alpha = 0.2$ model decays more quickly. Not surprisingly, the linear model has an exponential decay envelope, while the $\alpha = 0.2$ model has a nearly linear envelope, a property of Coulomb damping.

In the response of the second mode shape, the differences between the damping models are more clearly seen. The decay envelopes still transition from exponential to linear, but the rate of decay of the four models is significantly different. The models with larger α values damp out much more quickly in the second frequency. Also, the models with higher damping forces in the second mode generate vibration in the first mode of the structure, a phenomenon not associated with proportional damped systems. Essentially, the resisting forces from the dampers want to force the column to deform in the first mode shape and not the second.

More insight on the model's behavior can be gained by looking at the equivalent viscous damping ratios of the response. For each curve shown in the mode 1 response, the equivalent damping ratio is calculated between all successive peaks using the logarithmic decrement

method. These “instantaneous” damping ratios are plotted against peak height in Figure 4.

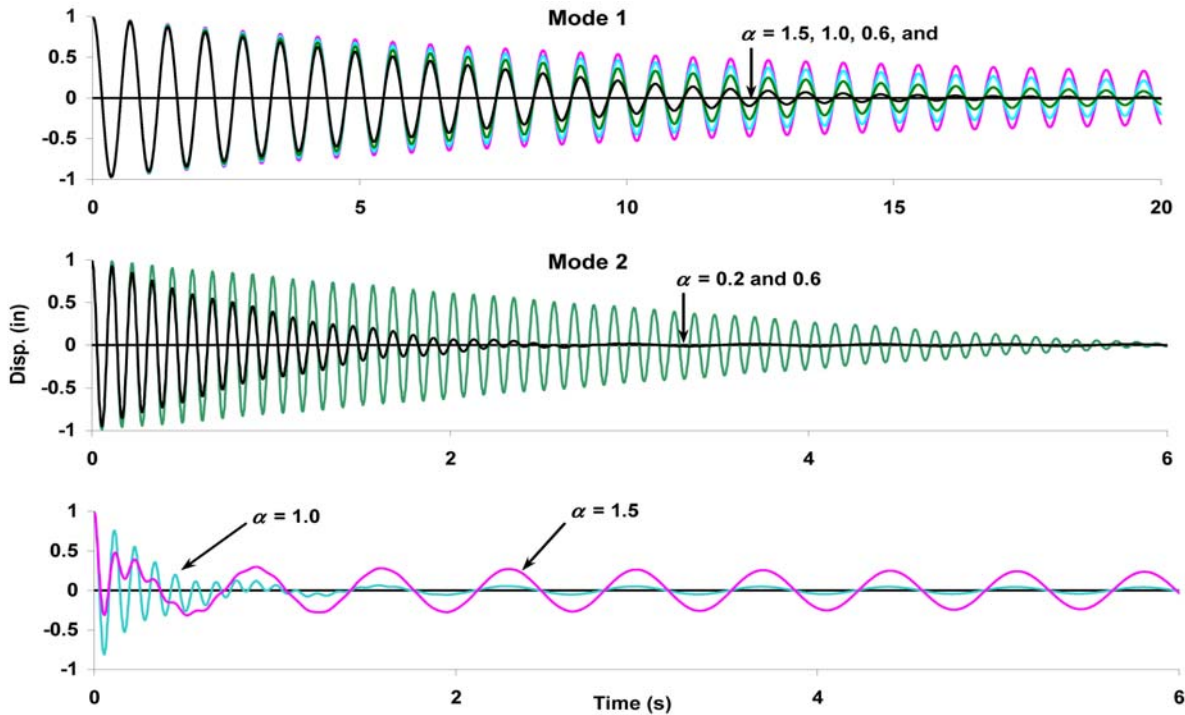


Figure 3. Lateral column displacements for free vibration in modes 1 and 2.

The figure shows that initially, all four models have nearly the same damping ratio. As expected, the model with viscous dampers maintains a constant damping ratio, while the models with $\alpha < 1.0$ show an increase, and the model with $\alpha = 1.5$ shows a decrease in equivalent viscous damping as vibrations reduce. At very low vibration, the curves level off, and the vibration becomes viscous. This leveling off is a result of the linearization of the nonlinear model at small velocities.

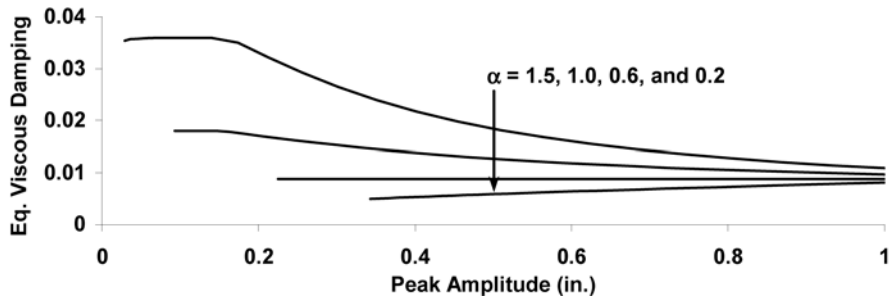


Figure 4. Equivalent viscous damping ratios.

The evolutionary aspects of the approach is based on rules which may be used to transform the damping behavior from one form to another. For example, in concrete structures, the damping is initially quite low and may be represented by linear viscous models. However, as

microcracks develop in the member, the effective damping will increase as the energy dissipation mechanism changes from viscous to frictional. However, under repeated cyclic deformation the ability of the system to dissipate energy will degrade as the coefficient of friction along crack planes is reduced. One of the goals of the research described herein is to develop realistic rules for modeling the evolutionary behavior.

Multiscale Model

Engineering materials dissipate dynamic energy within their material microstructure. The dissipated energy is quantified as the area enclosed by the load-displacement curve (Fig. 5a). Hysteretic damping models exist for many common engineering materials, including concrete in compression (Madeo 2006) and structural steel (Lazan 1968). It is the goal of this study to demonstrate, for a single degree of freedom system, how experimentally obtained hysteretic damping models can be implemented as an alternative to linear viscous damping.

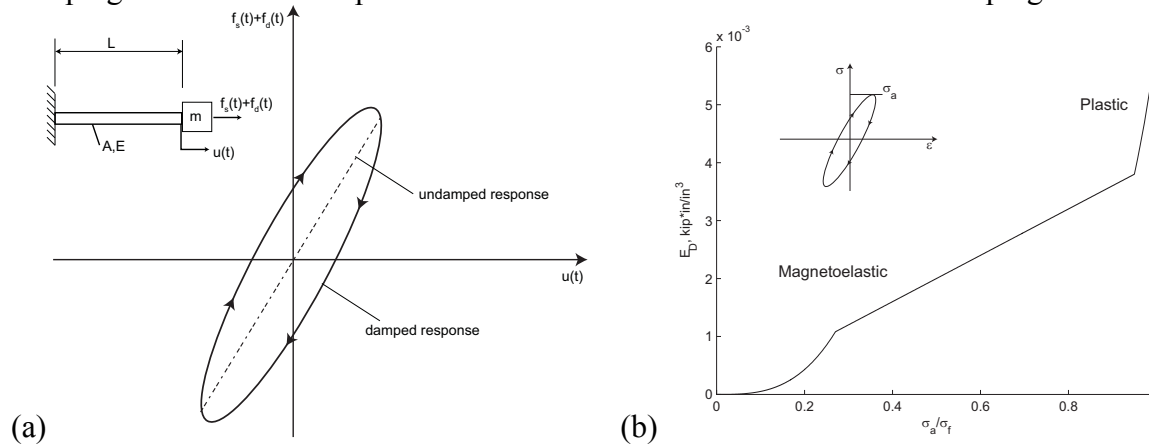


Figure 5. (a) Hysteretic damping and (b) Damping energy per hysteresis cycle for steel

For a single degree of freedom system, the damped free vibration dynamic equilibrium equation at time t is

$$f_i(t) + f_d(t) + f_s(t) = 0 \tag{3}$$

The dissipated energy from damping is represented as a force f_d , which acts in opposition to the inertial force, f_i . (The spring force is $f_s=ku$ where k is the axial stiffness, AE/L .) Typically linear viscous damping is assumed to derive f_d , ie. $f_d=c\dot{u}$, where \dot{u} is the velocity and c is a damping coefficient derived from experiments. Viscous damping is independent of the displacement amplitude, u , which is inconsistent with experimental observations for structural materials (Dowling 2007) and field measurements of damping in full scale structures (Tamura and Yoshida 2008). This inconsistency serves as the impetus for studying material damping laws (Fig. 5).

Ferromagnetic materials such as steel dissipate dynamic energy through atomic interaction of their crystalline microstructure. When the cyclic stresses on a volumetric element of a structural component are small relative to the yield stress, magnetoelastic damping is the dominant energy dissipating mechanism, resulting from the movement of dislocations and

sliding of grain boundaries in the crystalline microstructure of steel. As the stress level increases above the proportional limit toward the yield stress, plastic strain damping initiates with the slippage of crystal planes, a precursor to gross plastic deformation beyond the yield stress. The quantity of dissipated energy per unit volume of material over a load-deformation cycle, E_{dv} , with units of kip·in./in³, is approximated as (Lazan 1968)

$$\begin{aligned}
 E_{dv} &= 0.06 \left(\frac{\sigma_a}{\sigma_f} \right)^{3.07} & 0 < \frac{\sigma_a}{\sigma_f} \leq 0.27 \\
 E_{dv} &= 0.004 \left(\frac{\sigma_a}{\sigma_f} \right) & 0.27 < \frac{\sigma_a}{\sigma_f} \leq 0.95 \\
 E_{dv} &= 0.006 \left(\frac{\sigma_a}{\sigma_f} \right)^{8.9} & \frac{\sigma_a}{\sigma_f} > 0.95
 \end{aligned} \tag{4}$$

Note that Eq. 4 has been modified slightly from Lazan's original equation to provide a continuous function for E_{dv} through all stress levels considered. The variation in E_{dv} with applied stress is represented graphically in Fig. 5b, with the peak positive stress in a cycle defined as σ_a , and where σ_f is the fatigue stress for steel, typically taken as $\sigma_u/2$, where σ_u is the ultimate tensile strength of steel. The energy dissipated per cycle for the hysteretic model is different from a linear viscous model, because the damping is amplitude dependent, i.e. the damped energy per load-deformation cycle is dependent upon the applied stress at every unit volume of material in a structure. Lazan's equation suggests that when the stress is zero on a unit volume of material at time t , the instantaneous damping energy dissipated is also zero which is consistent with observed material damping (Clough and Penzien 1975).

Dynamic simulations are typically conducted assuming viscous damping. But what if instead a material damping law, i.e. Eq. 4, is used to simulate dynamic response? A proposed methodology employing material damping in lieu of viscous damping is derived herein for solving the dynamic response of a damped single degree of freedom system. An example problem — the damped axial free vibration response of a (massless) steel bar with mass m at its tip (inset of Fig. 5a), is performed to demonstrate the viability of the approach.

The classical finite difference solution algorithm for the damped free vibration of a single degree of freedom is (Chopra 2001):

$$m \frac{u_{i+1} - 2u_i + u_{i-1}}{(\Delta t)^2} + c \frac{u_{i+1} - u_{i-1}}{2\Delta t} + ku_i = 0 \tag{5}$$

where Δt is the length of time step i . If the viscous damping force in Eq. (5) is replaced with a general instantaneous damping force, f_{di} , applied at time step i , then:

$$m_i \frac{u_{i+1} - 2u_i + u_{i-1}}{(\Delta t)^2} \pm f_{di} + ku_i = 0 \tag{6}$$

Dynamic response is degraded as f_{di} is added or subtracted to act against the inertial force, i.e.

the first term in Eq. 6.

The damping force, f_{di} , and the dissipated energy over the time step, e_{di} , are related through the definition of instantaneous internal strain energy (Ugural and Fenster 2003):

$$e_{di} = \int_V \sigma_{di} \varepsilon_{di} dV \quad (7)$$

where σ_{di} and ε_{di} are the stress and strain in a unit volume of material caused by f_{di} . For an axially loaded bar (see inset of Fig. 5), the cross-sectional area A is constant, $\sigma_{di}=f_{di}/A$ and $\varepsilon_{di}=\sigma_{di}/E$, resulting in:

$$e_{di} = \frac{f_{di}^2 L}{AE} \quad (8)$$

The instantaneous damping energy is assumed equivalent to the energy dissipated over Δt in a hysteretic cycle with period T_n :

$$e_{di} = \frac{\Delta t}{T_n} \int_V E_{dvi} dV \quad (9)$$

The quantity E_{dvi} is calculated at each time step with Eq. 4 and the stress at each time step, σ_{di} . For the case of the vibrating axial bar with a constant cross-section, Eq. 9 simplifies to:

$$e_{di} = \frac{\Delta t}{T_n} E_{dvi} AL \quad (10)$$

Combining Eq. 10 and Eq. 8 and solving for f_{di} of the axially vibrating bar:

$$f_{di} = \pm A \sqrt{\frac{\Delta t}{T_n} E_{dvi} E} \quad (11)$$

The damped free vibration response for a steel bar with cyclic natural frequency of 10 Hz ($\omega_n=62.8$ rad/sec) is presented in Fig. 6a. Two initial displacements corresponding to axial stresses ratios of $\sigma(0)/\sigma_f=0.10$ and $\sigma(0)/\sigma_f=0.50$ are considered. The responses vary based on the initial displacement (stress), demonstrating that the influence of damping is stress amplitude dependent when employing the hysteretic damping model in Eq. 4. The free vibration response at an initial stress amplitude of $\sigma(0)/\sigma_f=0.10$ is most consistent with the viscous damping free vibration response curve assuming a viscous damping ratio for steel of $\xi=0.005$. The similarity between the viscous damping and experimentally based hysteretic damping response occur even though the damping force f_d loops (Fig. 6b) are shaped differently. The f_d vs. u response for the material damping law resembles a bow tie, with zero damping occurring when the bar displacement is zero. Also note that the distance between the f_d loops varies nonlinearly as axial stress in the bar decreases for the hysteretic model (consistent with Fig. 6b), whereas f_d decreases at a constant rate for viscous damping.

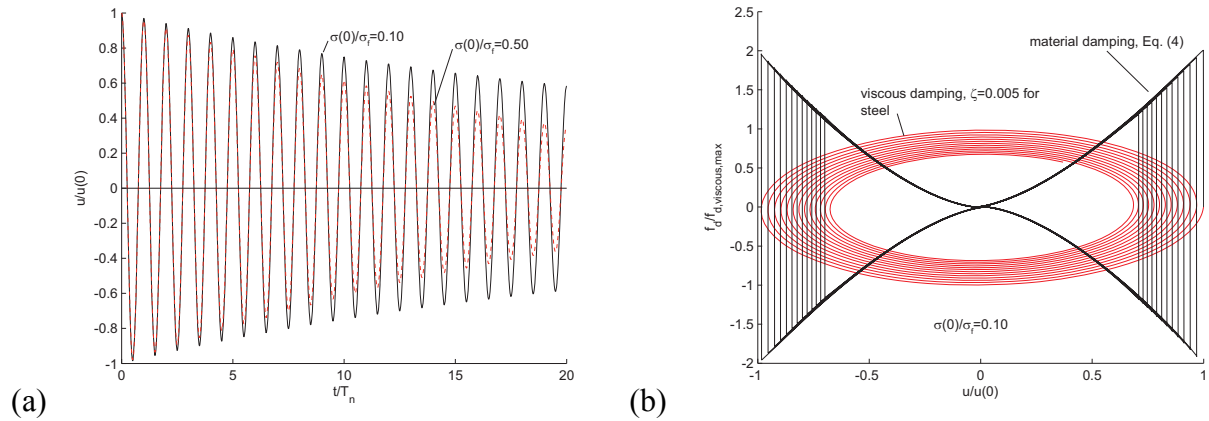


Figure 6 (a) Free vibration response is amplitude dependent with the hysteretic damping model and (b) damping force function shape for viscous damping and hysteretic damping

The steel bar response demonstrates that alternative damping models to viscous damping can produce dynamic responses consistent with physical observations. Future work is planned to validate the SDOF results presented in Fig. 6 with experiments. Also, the fundamental concept of a multiscale damping approach — where experimentally derived material damping models are integrated into response simulations through elastic strain energy relationships — will be extended to damping from flexural and shear deformation. It is envisioned that the multiscale approach could also be integrated with the evolutionary damping scheme presented earlier in the paper. The result will be a framework which integrates realistic, mechanics-based amplitude dependent damping behavior into nonlinear computational dynamic simulations of multi-degree of freedom structural systems.

Conclusions

Due to the uncertainties associated with damping behavior in structural systems, current modeling procedures rely on simplified assumptions and inaccurate representations of behavior. The common practice of using global linear viscous damping does not account for different behaviors in the various components within a system, or changing behavior of the components. The discrete-spring model presented in this paper allows a variety of phenomenological damping behaviors to be incorporated. The evolutionary model accounts for variations in damping through the use of an exponential function of velocity, where the time varying damping coefficient and nonlinearity exponent dictate the response. This allows the damping characteristics to be updated as the structural behavior changes. In the analysis, both amplitude and frequency affect the response, which is a characteristic not developed in linearly viscous damping. The major challenges associated with this method are determining when and how the damping coefficient exponent will change during the response. Finding these shifts in behavior will likely need to be developed with experimental testing on the material and structural level.

The multiscale model uses the behavior of material at the microscopic level to represent the changes in the structure that relate to the damping. By using experimental hysteretic damping

models, the area enclosed by the hysteretic loop can be representative of the damping force and can be determined for any response. This eliminates the global and linear aspect of current damping procedures, because the energy can be found at any location in the system under any behavior, whether linear or nonlinear. The results show that damping behavior at low amplitudes is similar to linear viscous damping but diverges at higher amplitudes when the response becomes nonlinear. This model relies on experimental behavior, which becomes both an advantage and disadvantage. While the results produced by the model are more representative of realistic behavior, the model cannot be used without the experimental relations.

References

- Bernal, D. (1994). "Viscous Damping in Inelastic Structural Response." *Journal of Structural Engineering*, 120(4), 1240-1254.
- Charney, F. A. (2008). "Unintended Consequences of Modeling Damping in Structures." *Journal of Structural Engineering*, 134(4), 581-592.
- Chopra, A., K. (2001). *Dynamics of Structures, 2nd Edition*, Prentice Hall, Upper Saddle River.
- Chrisp, D. J. (1980). "Damping Models for Inelastic Structures," Master of Engineering Report, University of Canterbury, Christchurch, New Zealand.
- Clough, R. W., and Penzien, J. (1975). *Dynamics of Structures, 1st Edition*, McGraw-Hill, New York.
- Dowling, N. E. (2007). *Mechanical Behavior of Materials*, Pearson Prentice Hall, Upper Saddle River.
- Hall, J. F. (2006). "Problems Encountered from the use (or misuse) of Rayleigh Damping." *Earthquake Engineering and Structural Dynamics*, 35(5), 525-545.
- Hanson, R. D., and Soong, T. T. (2001). *Seismic Design with Supplemental Energy Dissipation Devices*, Earthquake Engineering Research Institute, Oakland, CA.
- Lazan, B. (1968). *Damping of Materials and Members in Structural Mechanics*, Pergamon Press, New York.
- Madeo, A. (2006). "Effect of Micro-Particle Additions on Frictional Energy Dissipation and Strength of Concrete [MS Thesis]," Virginia Tech, Blacksburg, VA.
- Powell, G. H. (2008). Personal Communication.
- Tamura, Y., and Yoshida, A. "Amplitude Dependency of Damping in Buildings." *Proceedings of the 2008 Structures Congress*, Reston, VA.
- Ugural, A. C., and Fenster, S. K. (2003). *Advanced Strength and Applied Elasticity, Fourth Edition*, Prentice Hall, Upper Saddle River, NJ.